Preferred citation: A. Jäsberg and M. Kataja. New experimental results on the flow regimes in closed channel flows of wood fibre suspensions. In **Advances in Pulp and Paper Research, Oxford 2009**, *Trans. of the XIVth Fund. Res. Symp. Oxford, 2009*, (S.J. I'Anson, ed.), pp 161–180, FRC, Manchester, 2018. DOI: 10.15376/frc.2009.1.161.

NEW EXPERIMENTAL RESULTS ON THE FLOW REGIMES IN CLOSED CHANNEL FLOWS OF WOOD FIBRE SUSPENSIONS

Ari Jäsberg[1,2] (ari.u.jasberg@jyu.fi) and Markku Kataja[1]

[1] Department of Physics, P.O. Box 35 (YFL), FI-40014 University of Jyväskylä, Finland
[2] VTT, P.O. Box 1603, FI-40101 Jyväskylä, Finland

ABSTRACT

We consider here the behaviour of wood fibre suspension with fibre concentration above that of sedimentation in a pressure driven flow in a straight pipe with smooth walls. The flow behaviour can be roughly divided in two main regimes: the plug flow regime that occurs at low flow rates and the drag reduction regime that occurs at high flow rates. We utilized new experimental methods in order to gain more detailed understanding on the flow behaviour of wood fibre suspensions, and especially on the relevant physical phenomena inducing such behaviour. In addition to carrying out conventional loss experiment, the velocity profiles across the pipe were measured using pulsed ultrasound velocimetry (PUDV) techniques, and the thickness of the lubrication layer in fully developed flow was measured using a laser-optical device. Based on our direct measurements, we were able to indentify five different flow regimes in suspension flows. In addition, we refined the qualitative picture of these flows in relation to the forming of fibre plug and to the physical phenomena taking place in transition from one flow regime to another one.

1 BACKGROUND

According to Duffy, the flow behaviour of wood fibre suspensions can be roughly divided in two main regimes: the plug flow regime that occurs at low flow rates and the drag reduction regime that occurs at high flow rates [1, 2]. Within the plug flow regime the fibre phase moves as a continuous fibre network with solid like properties and with no shearing motion. In this regime, the loss is high compared to that of the carrier fluid (usually water) at the same flow rate. Furthermore, the dependence on flow rate of loss can be quite complicated. In some cases the loss may decrease with increasing flow rate. In the drag reduction regime, the fibre network is partly or entirely broken into flocs that undergo turbulent and shearing motion. Characteristic to this region is that the frictional loss may be below that of a pure carrier fluid.

These qualitatively different main regimes can be divided into several subregimes. If the pressure gradient applied to the pipe is below some threshold value that depends on fibre type and consistency, the fibre plug does not move at all and the motion of the carrier fluid is described as a flow through porous medium. Above the threshold pressure gradient, also the fibre plug is set into motion. The fibres are first in a direct contact with the wall inducing high shear stress (high loss). As the flow rate is increased, a plug flow behaviour is preserved, but a thin layer of pure water (a lubrication layer) is created next to the wall. Characteristic to this flow regime is that the wall friction is approximately constant, and may even decrease with increasing flow velocity. As the flow rate increases further, turbulent flow appears near the walls and the fibre plug begins to break from its outer surface. Thus, in this mixed flow regime a turbulent fibre annulus surrounds a rigid fibre plug in the middle of the pipe. At some point, frictional loss falls below that of the carrier liquid and drag reduction regime is obtained. As the flow rate is still increased, the solid fibre core gradually vanishes indicating fully turbulent or fluidized flow regime. Here, the loss typically approaches the pure fluid curve asymptotically as the flow rate is increased. This quite generally accepted view on the different flow domains was originally based on loss measurements, visual observations of the flow near the pipe wall and on velocity profile measurements made at turbulent region using a specific annular-purge impact probe [1, 2].

It should be noticed that the partitioning of the flow rate domain to two main regimes by Duffy was motivated mainly by dimensioning purposes. For the practical design purposes the results of extensive loss studies have traditionally been published in a graphical form, see *e.g.* Ref. [3]. These graphical correlations have been used, *e.g.*, to estimate the frictional losses for pipe diameters that were not included in the original measurement. Later, specific

design equations have been developed for the regime before the maximum in the loss curve, see Ref. [4] for a extensive review and evaluation of these equations. Møller and Duffy have derived an empirical loss correlation in the transitional regime [5]. There are design procedures that have been developed to cover a wide range of flow velocities and consistencies. One of these procedures is documented in Ref. [6].

In this work, we utilized new experimental methods in order to gain more detailed understanding on the flow behaviour of wood fibre suspensions, and especially on the relevant physical phenomena inducing such behaviour. In addition to carrying out conventional loss experiment, the velocity profiles across the pipe were measured using pulsed ultrasound Doppler velocimetry (PUDV) techniques, and the thickness of the lubrication layer in fully developed flow was measured using a laser-optical device. The results have been used in modeling the loss behaviour both in plug flow regimes and in turbulent regimes[7]. We do not report here comprehensive results, but rather demonstrate the capabilities of the experimental methods used in this work.

2 EXPERIMENTAL WORK

In this experimental work, suspensions consisting of water and chemically released pine or birch fibres were studied. The physical dimensions of fibres were measured with a commercial fibre analyzer at Technical Research Center of Finland (VTT) [8]. In the analyzer fibres are aligned between two glass windows and imaged with a CCD camera, after which the fibre dimensions are calculated with image analysis. The results include, *e.g.* distributions for the fibre length and width, and the averages of these distributions. The total mass of dry fibres is measured before the analysis, thus the coarseness of fibres can be calculated, too. The results for the average physical dimensions and coarseness are presented in Tab. 1. Also shown in the table is the aspect ratio $A = L/d$ calculated from the average physical dimension.

The flow experiments were made in a laboratory-scale acrylic flow loop with pipe diameter 40 mm. The flow was driven by a centrifugal pump, and the flow rate was measured using a magnetic flow meter. The flow loop was equipped with a differential pressure transducer for loss measurement. The velocity profiles across the pipe were measured using pulsed ultrasound Doppler velocimetry (PUDV). In a separate experiment, the thickness of the lubrication layer in the plug-flow regime was measured optically using a collimated laser beam guided inside the flow channel, and measuring the light scattered by fibres.

Table 1. Experimental results for the average fibre length L, the average fibre width d, and the coarseness of fibres ω. Also shown is the aspect ratio $A = L/d$ calculated from the physical dimensions.

Species	*# fibres analyzed*	*L [mm]*	*d [μm]*	*A=L/d*	*ω [μg/m]*
Pine	20000	2.0	27.7	71	147
Birch	45000	0.90	21.0	43	109

2.1 Ultrasound velocimetry

The velocity profile across the pipe was measured using PUDV. The measurement is based on using a transmitter to send short ultrasound pulses through the pipe wall and into the flow. Target particles (fibres) moving with the flow reflect the sound which is detected by the transmitter. The distance of the particle is found by the time-of-flight method using the known velocity of sound, and the velocity of the particle is calculated from the cross-correlation between the echoes from consequent pulses. Notice that the device thus measures the velocity component in the direction of the ultrasound beam. Within the present measurement, an ultrasound transmitter with the emitting frequency of 4 MHz was used. The angle between the axis of the probe (the direction of ultrasound beam) and the pipe wall was set to $\theta = 85°$. The duration of a single ultrasound pulse was selected as 4 wavelengths corresponding to a length 1.5 mm in water with the velocity of sound 1500 m/s. The repeating frequency of pulses was set to 15.6 kHz, thus the time delay between the emissions of two consequent pulses was 64.0 μs while a single pulse lasted only for 1.0 μs. The echo signal was sampled in 54 gates (windows) corresponding to 54 depth values with spacing 0.75 mm in the direction of ultrasound beam. A series of 32 pulse emissions was used to construct a single velocity profile u_{us} (z_{us}, t), and 3000 profiles were collected during 20 seconds. Here u_{us} is the velocity component in the direction of the ultrasound beam and z_{us} is the distance along the beam axis from the front wall of the flow channel. Velocity profiles $u(z, t)$ were calculated, where $u = u_{us}/\cos\theta$ is the velocity component in the direction of the pipe axis and $z = z_{us}/\sin\theta$ is the perpendicular distance from the front wall of the flow channel. The mean velocity profile $\bar{u}(z)$ was calculated as the average of these 3000 individual profiles

$$\bar{u}(z) = < u(z,t) >, \tag{1}$$

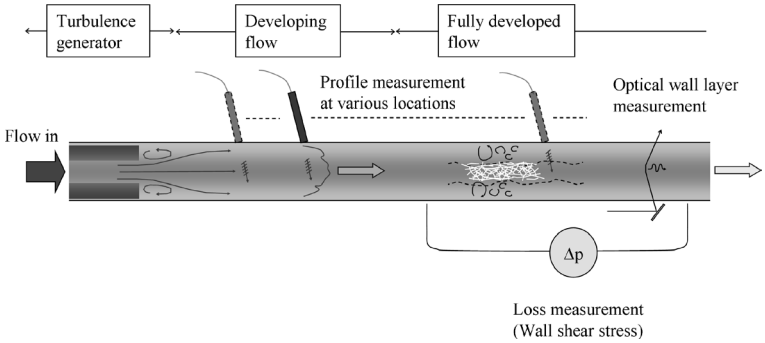

Figure 1. Schematic illustration of the experimental arrangement for fibre suspension flow in a straight pipe after a turbulence generator.

where <> denotes average over 3000 separate velocity profiles, *i.e.* average over time.

The PUDV -method was applied to study the flow in a straight pipe of diameter is $D = 40$ mm and length $L = 3.2$ m with a constriction block of inner diameter 20 mm and length 0.25 m placed inside the entrance part of the pipe, see Fig. 1. The resulting backward facing sudden step provided by the exit end of the constriction block generates a recirculation zone and a strong turbulent field in the downstream part of the pipe. The velocity and fluctuation profiles through the pipe diameter were measured at 18 fixed locations after the constriction block for different flow rates varied between 0.6 and 3.5 l/s. The first measuring point was located at distance 0.2 m and the last point at distance 2.6 m from the step. The measurement zone thus includes portion of the pipe, downstream of the recirculation zone, where the flow is already reattached to the pipe walls, takes place in a decaying turbulent field and approaches a fully developed condition towards the end of the pipe. In this experiment birch fibre suspension at consistency 1.0% was used.

In order to characterize the turbulent state of the flow, we look at a time averaged correlation function of velocity fluctuations

$$g(z, z') = < \delta u(z,t)\delta u(z',t) >, \tag{2}$$

where $\delta u(z, t) = u(z, t) - \overline{u}(z)$ is the fluctuating velocity component. In an ideal case we would define the local intensity of the velocity fluctuations at the depth $z = z_0$ as the value $g(z_0, z_0)$. In reality, however, the individual velocity profiles given by the PUDV method suffer from a noise intrinsic to the measuring principle. This noise contributes to the intensity given by Eq. (2), and

for weak fluctuations it dominates the intensity totally obscuring the actual fluctuations of the flow. It appears, however, that we can eliminate the noise from the results. To that end, we consider the cross-section $g(z_0 - \delta z, z_0 + \delta z)$ for a fixed value of depth z_0. This cross-section is almost Gaussian except for the center $\delta z = 0$ where there are a few points of large values due to the intrinsic noise. We exclude these points and fit in the rest of the data a Gaussian function

$$f(\delta z) = I_T \exp(-(\delta z/\lambda_{\delta u})^2), \tag{3}$$

where the parameter I_T gives the corrected intensity for the velocity fluctuations at the depth z_0.

2.2 Laser-optical lubrication layer measurement

The thickness of the lubrication layer was measured in a fully developed flow with a special-purpose laser-optical device. In the device, a collimated laser beam was guided inside the acrylic flow channel, see Fig. 2. The laser beam was generated with a 5 mW helium-neon laser (wave length $\lambda = 623$ nm), and guided through an beam expander that increases the beam diameter from 1 mm to 10 mm. The expanded beam was collimated with a focussing lens $f = 100$ mm, and the resulting focal waist of the beam was approximately

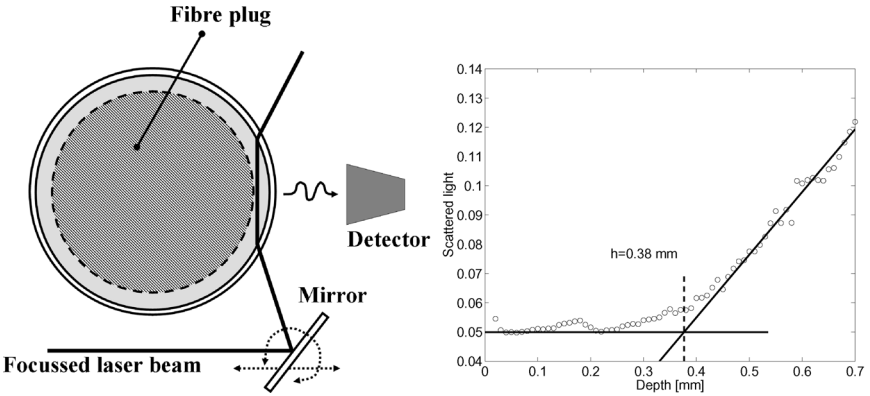

Figure 2. Left: the principle of laser-optical measurement of the lubrication layer. Right: the intensity of the laser light scattered by pine fibres at consistency 0.5% (by weight) as a function of distance from the pipe wall at flow rate $Q = 0.54$ l/s. The crossing point of two fitted lines defines the thickness of the fibre free lubrication layer.

10 μm in diameter. The light scattered from fibres traversing the beam was detected by an optical sensor placed just outside the pipe wall, and having a narrow horizontal field of view through the pipe wall into the focal point of the beam. The straight pipe sections upstream and downstream of the measuring point were approximately 2.7 m and 0.5 m, respectively. For each flow rate, 10000 light intensity values were collected at a sampling rate adjusted according to the mean flow velocity such that the distance between consequent measuring points in the moving fibre plug was approximately 1 mm. Thus a length 10 m of the suspension flowing in the pipe was measured to give an adequate and statistically similar set of measurements for all flow rates.

Figure 2 shows an example of results obtained by the laser-optical device discussed above. In the figure, shown is the mean intensity of scattered light as a function of the laser beam depth inside the pipe. The result is for pine fibre suspension at consistency 0.5% (by weight) and flow rate 0.54 l/s, where the flow is well in the plug flow regime. The layer of pure water is indicated by a region next to the wall of nearly constant, low intensity. As the beam enters the fibre plug, the intensity starts to increase with the beam depth more or less linearly. The thickness of the lubrication layer is defined as the crossing point of the two straight lines fitted to the data points in the constant intensity region and in the increasing intensity region as indicated in Fig. 2 (right). In the flow condition shown, the thickness of the lubrication layer is thus estimated to be 0.38 mm.

3 RESULTS

3.1 Transient phenomena in developing flow

Figures 3–5 show the mean velocity and turbulent intensity profiles at various locations along the pipe for flow rates 0.6 l/s, 1.9 l/s, and 3.5 l/s. At all flow rates used, the turbulent intensity immediately after the sudden expansion is very high indicating that the suspension is in a fluidized state where the fibre phase is broken into small flocs that undergo turbulent motion. The turbulent intensity is highest in the middle of the pipe and decreases rapidly with distance x as the fluctuations of the fibre phase cease. At low flow rate (see Fig. 3), the fibre phase finally forms a continuous network that spans through the pipe, except of a thin fibre free lubrication layer that may be formed at the walls. It should be noticed that this layer can not be observed with the PUDV techniques, but is clearly observable with the laser-optical measurement, see Fig. 6. The shape of the mean velocity profile undergoes only minor change along the pipe, being plug-like turbulent profile immediately after the

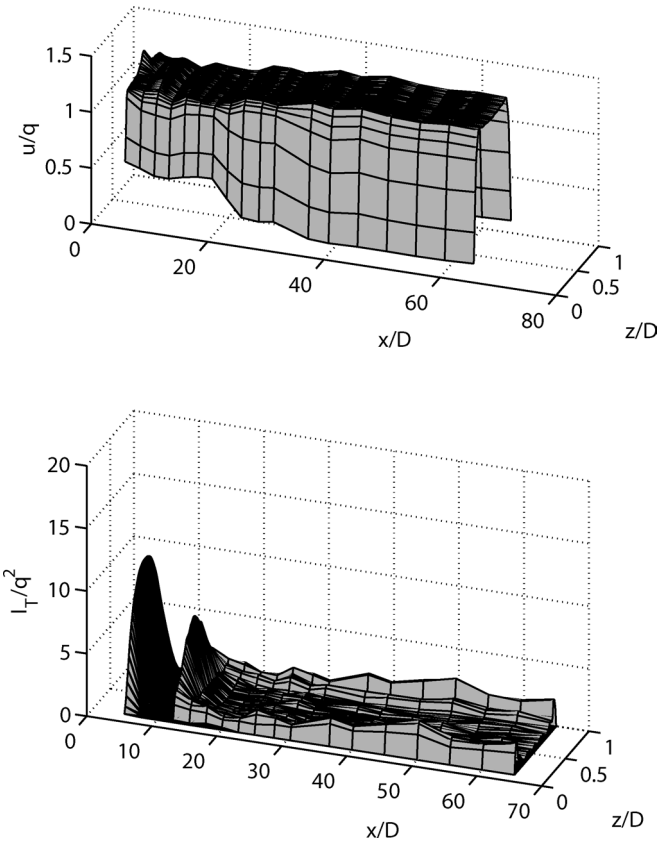

Figure 3. The measured mean velocity profile (top) and turbulent intensity profile (bottom) for birch fibre suspension at the consistency $c = 1.0\%$ (by weight) after the sudden expansion with area ratio 1:4. Flow rate is $Q = 0.6$ l/s and the the corresponding Reynolds number calculated with the properties of water is $\mathrm{Re_w} = 22000$. The insert in right figure shows the measured turbulent intensity multiplied by a factor 100 for clarity in the latter part of the pipe. Here, x is the downstream distance from the sudden expansion, z is the distance from the inner surface of the pipe wall along the horizontal pipe diameter, q is the average flow velocity, and D is the pipe diameter.

recirculation zone and turning into a plug-like steady profile further downstream where the flow approaches fully developed condition. The developed profiles shown in Fig. 3 are typical to plug flow regime.

At moderate flow rate (see Fig. 4) the behaviour is similar to that with low

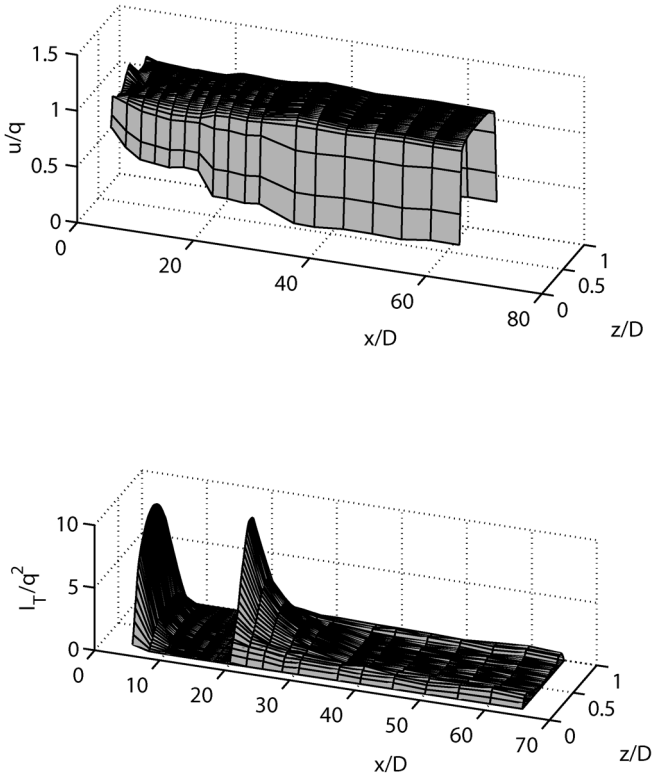

Figure 4. As Fig. 3, but for Q = 1.9 l/s (Re_w = 60000).

flow rate. However, the overall turbulent intensity is higher and the high intensity region extends further downstream. In addition, the increased wall friction now prevents fibres from forming continuous network near the walls. Instead, a turbulent annulus remains near the walls and a continuous network is formed only at the core. This is seen as the turbulent intensity maxima near the walls and a slightly more rounded mean flow profile in the developed flow region. Here, the developed flow is typical to the mixed flow regime.

At the highest flow rate (see Fig. 5), the initial turbulent intensity is still higher and extends still further downstream. The turbulence induced by strong wall friction now prevents formation of continuous fibre network throughout the pipe. The suspension remains fully fluidized also in the developed flow and is thus in the turbulent flow regime. Although the mean velocity and turbulent intensity profiles in the developed flow region appear

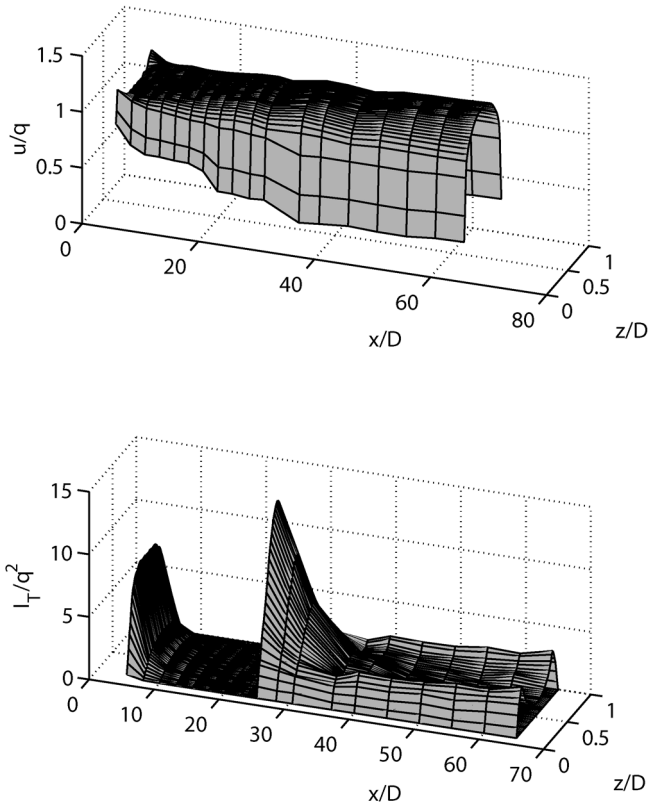

Figure 5. As Fig. 3, but for Q = 3.5 l/s (Re_w = 110000).

quite similar to those for ordinary turbulent flow of simple fluids, a closer examination of the mean velocity profile reveals marked differences to the conventional logarithmic law behaviour (see Fig. 7).

So far we have been able to identify three main flow regimes, namely plug flow regime, mixed flow regime and fully turbulent flow regime. In what follows, by looking at the fully developed flow and the results given by the laser-optical device, we will be able to further classify the plug flow regime into three subregimes.

3.2 Fully developed flow

3.2.1 Thickness of the lubrication layer

In Fig. 6 shown are the measured values of layer thickness as a function of mean flow velocity at low consistencies just above the sedimentation consistency. The measured layer thickness is shown only for those flow velocities at which a well defined finite thickness value could be found. Especially with the present measuring techniques, the lubrication layer could not be observed at very low flow rates. It appears that in each case, the regime where the lubrication layer was not found coincides with the low flow rate domain where the

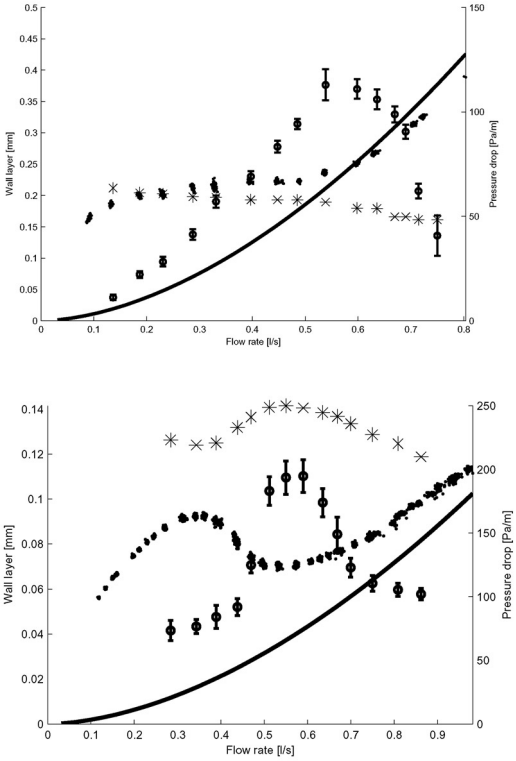

Figure 6. Measured pressure drop (small dots) and wall layer thickness (open circles) versus flow rate for pine suspension at consistency 0.5% (top) and birch suspension at consistency 1.0% (bottom). Solid line is the pressure drop of water, and stars give the thickness of the viscous sublayer ($y^+ = 5$) for water at each value of loss.

loss increases with flow rate. This domain is naturally identified as the plug flow regime with direct fibre-wall contact (regime I in Fig. 8). An observable lubrication layer appears at the flow rate corresponding to the local maximum in the loss curve (birch) or to the point where the loss curve levels off (pine). Above that flow rate, the measured value of the lubrication layer thickness first grows with flow rate, reaches a maximum and then starts to decrease. In general, the thickness decreases with consistency and the location of maximum point becomes less definite. The flow rate corresponding to the maximum layer thickness (where observable in the data) falls approximately at the same point, where the loss curve again starts to grow. This domain is identified as the plug flow regime with lubrication layer (regime II in Fig. 8). The observed decrease of the layer thickness after the maximum is most likely due to incipient turbulence, *i.e.* turbulence in the fluid phase (that was not observed with the present methods). This turbulence is not yet strong enough to cause macroscopic breakage of the fibre network, but only to bend and dislodge individual fibres that are loosely bound to the fibre plug surface. These fibres can then be randomly displaced towards the pipe wall by fluctuations of fluid velocity, and thereby cause increased light scattering as they traverse the laser beam. The apparent decrease of lubrication layer thickness may thus be explained by dispersion of the fibre plug surface layer due to fluid phase turbulence. In this region the measured lubrication layer thickness decreases and pressure loss increases but macroscopic rupture of fibre plug is not yet observed.

3.2.2 Velocity profiles in the mixed and turbulent flow regimes

Figure 7 (top) shows the mean velocity profiles of pine fibre suspension of consistency 1% for flow rate ranging from 1.5 l/s to 5.0 l/s. Due to noise caused by the wall-fluid interface, the velocity measurement by the PUDV method is not accurate below 1 mm from the wall, and those results are excluded from the profiles shown. A peculiar feature of the measured mean velocity at high flow rates is the S-shaped profile near the wall. (A similar result was obtained recently also by Xu and Aidun for rectangular channels [9].)

As in the case of Newtonian flows, parameterization of turbulent velocity profiles of fibre suspensions is best done by utilizing the standard non-dimensional wall-layer variables defined by

$$u^+ = u/u^\star \tag{4}$$

$$y^+ = yu^\star/\nu_\mathrm{f} \tag{5}$$

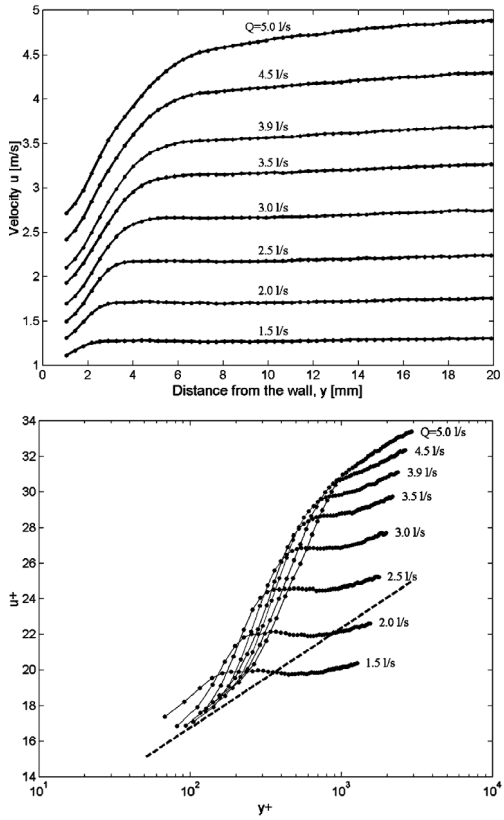

Figure 7. Top: mean velocity profiles of pine fibre suspension at consistency 1% as a function of distance from the pipe wall. The flow rate is varied from 1.5 l/s to 5 l/s where the flow is in the mixed or turbulent flow regimes. The centre line of the acrylic pipe is located at y = 20 mm. Bottom: mean velocity profiles expressed with standard non-dimensional wall-layer variables.

where $u^* = \sqrt{\tau_w/\rho_f}$ is the friction velocity, ρ_f and ν_f are the density and the kinematic viscosity of the fluid and τ_w is the wall shear stress obtained from the pressure drop measurements. Figure 7 (bottom) shows the same velocity profiles as Fig. 7 a) but redrawn in the dimensionless variables. Also shown is the standard logarithmic velocity profile for turbulent Newtonian flow, namely:

$$u^+ = \frac{1}{\kappa}\ln(y^+) + B \tag{6}$$

where the constants κ and B have the standard values 0.41 and 5.5, respectively [10].

A remarkable feature of the profiles shown in Fig. 7 is that there seems to exist a unique (approximate) envelope curve that corresponds to a limiting velocity profile shape as the flow rate approaches infinity. That envelope curve consists of a logarithmic near wall region where the profile coincides with that of Newtonian flow, a yield region where velocity gradient is higher than that of Newtonian flow, and a core region where the profile again is of the form given by Eq. (6) but with a value of constant B above that of Newtonian flows. The near wall region extends up to a distance scale $y^+ \sim 10^2$. Correspondingly, the core region starts at a distance scale $y^+ \sim 10^3$ and extends up to pipe axis.

4 DISCUSSION

4.1 Flow regimes

Based on the experimental results discussed above, the main qualitative features of flow of wood fibre suspensions in straight pipe are now summarized. Direct observation using various experimental methods suggests that one can divide the flow into five different regimes according to flow rate. These regimes are shown in Fig. 8.

In the plug flow regime with wall contact (regime I), the intensity of turbulence is high immediately after the source, and the suspension is in a fluidized state where the fibre phase is broken into flocs. The intensity of the turbulence decays rapidly downstream from the source, and the fibre phase forms into a continuous network. In this process, the turbulent energy of fibres is partly captured as the elastic energy of the network, which manifests itself as an elastic force that pushes fibres towards the pipe wall. On the other hand, solid objects (wood fibres in this case) immersed into a flow near a solid wall experience a so called lift force, a side force that may repell them away from the wall [11, 12, 13, 14, 15]. In this regime of low flow velocity, the elastic force is, however, large enough to keep the fibre plug in a contact with the wall. Thus the fibre network forms into a state that spans through the pipe, and no observable lubrication layer is found. The radial force balance of the fibre plug is maintained between the elastic force, the lift force, and a support force by the wall. The support force give rise to mechanical friction between the fibre plug and the pipe wall, increasing the loss.

The plug flow regime with lubrication layer (regime II) is quite similar to the regime I, with the exception that the lift force is large enough to keep the fibres away from the pipe wall, on the average. Thus the fibre network forms

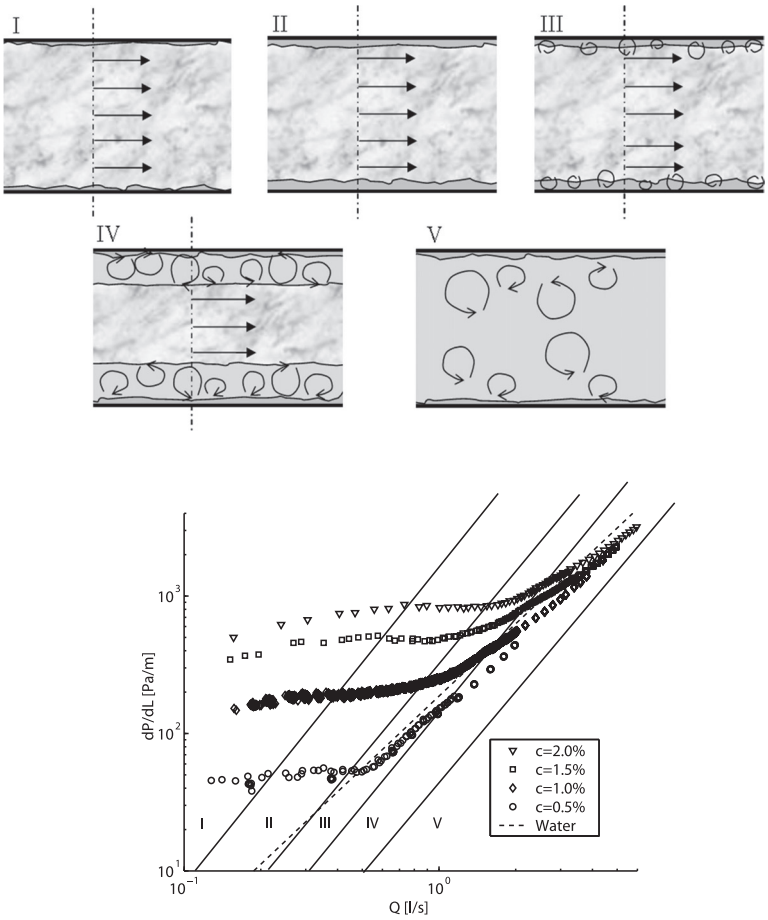

Figure 8. Top: The main regimes of fully developed flow of fibre suspensions. (I) Plug flow regime with direct fibre-wall contact, (II) plug flow regime with lubrication layer, (III) plug flow regime with incipient (fluid phase) turbulence, (IV) mixed flow regime and (V) fully turbulent flow regime. Bottom: flow regimes with loss data for pine fibre suspension at varying consistency.

into a state where there is a fibreless lubrication layer next to the pipe wall. The thickness of this layer increases with flow rate. Due to the lubrication layer, the loss saturates of may even decrease with increasing flow rate.

In the plug flow regime with smearing annulus (regime III) the loss increases approximately linearly with flow rate, and the behaviour of the

lubrication layer thickness is ambiguous. Fluctuations in the fluid phase (incipient turbulence) deform and disengage individual fibres on the surface of the fibre plug. These fibres are randomly displaced towards the wall into the lubrication layer by the fluctuations in the fluid velocity, which eventually renders the lubrication layer unobservable.

In the mixed flow regime (regime IV) the dependence on the flow rate of the loss is approximately quadratic. The turbulence induced by the high flow velocity and the strong wall friction prevents fibres from forming a continuous network near the walls. Thus the fibre plug is only formed at the core and a turbulent annulus remains at the walls.

In the fully turbulent regime (regime V) the turbulence created by strong wall friction prevents the formation of the fibre plug throughout the pipe, and the suspensions remains in a fluidized state. The transition from mixed flow regime IV into fully turbulent regime V is gradual and no sharp change in loss behaviour can be observed. The dependence on the flow rate of the loss remains close to quadratic in the transition, thus the exact flow rate at which the fibre plug core disappears can not be identified from loss data. This topic will be discussed in greater detail below utilizing the results from velocity profile measurements. At very high flow rates, the loss behaviour approaches that of pure carrier fluid.

Although the classification discussed above and depicted in Fig. 8 is very similar to those presented previously (see *e.g.* Ref. [1]), there are some subtle differences. In particular, the existence and nature of regime III and identification of the different flow regimes in the loss data are now more precisely defined. Notice also, that the present classification is based on direct experimental evidence on various features of the flow.

4.2 Transition between the regimes

Given the new profile information obtained by the PUDV method, the dynamics of the transition from the incipient turbulent regime via mixed flow regime to the fully turbulent regime (regimes III, IV and V in Fig. 8 can now been discussed in more detail. The incipient turbulence region most likely arises due to growth of the lubrication layer thickness until turbulent fluctuations of the fluid phase can exist between the wall and the fibre plug. This is supported by the results shown in Fig. 6, where the maximum layer thickness is $y^+ \sim 10$ for pine fibres and $y^+ \sim 4$ for birch fibres, *i.e.* close to the thickness of the viscous sublayer. The edge of the fibre plug is not sharp, however. Instead, a surface layer exists where the average fibre consistency increases from zero to some constant value within a distance scale set by a structural correlation length of the fibre network. Due to low fibre consist-

ency near the surface, the fluid phase turbulence is not effectively damped until well inside the plug. Consequently, the flow behaviour is dominated by fluid phase turbulence in a region that starts from the outer edge of the viscous sub-layer well inside the fibre free lubrication layer, and extends inside the fibre core a distance of the order of correlation length. This explains the observed behaviour that the velocity profile of fibres approach that of turbulent Newtonian fluid near the wall. Remember that the PUDV techniques could not be applied close enough to the wall such that the linear viscous sub-layer could be resolved.

As the flow rate is increased, turbulence production at the wall increases and fluctuations can prevail deeper in the fibre phase core preventing fibres from forming continuous network within some annular region. Well inside the core, fibre consistency is high leading to effective attenuation of turbulent fluctuations. The attenuation is most effective in the size scale of correlation length. On the other hand, the size scale of the largest eddies, that contain most of the turbulent energy and that are most effective in momentum transfer (i.e. in generating turbulent friction) is set by the distance from the wall. An immediate consequence of the arguments given above is that at a distance of the order of correlation length from the wall, the largest eddies possible at that distance, are effectively attenuated by the fibres. Consequently, the turbulent friction is attenuated leading to the yield layer characterized by increasing velocity gradient and the S-shaped profile shown in Fig. 7. (Obviously, this conclusion is based on an assumption that the friction is dominated by turbulence.) The existence of the yield layer, is the origin of the drag reduction phenomenon – although within the present reasoning that region could more accurately be described as the 'region of flow enhancement'.

As the flow rate is further increased, the turbulent production still increases and the turbulent annulus can diffuse deeper in the fibre core. Entering further away from the wall leaves space to larger eddies that are not anymore attenuated very effectively. As a consequence, the core region can finally remain turbulent due to eddies larger than correlation length. Furthermore, the large scale end of the turbulent spectrum near the pipe centre can become similar to that of pure fluid. At very high flow rates the turbulent momentum transfer and consequently the mean velocity gradient approaches that of turbulent Newtonian flow. That would explain the limiting value of slope in the logarithmic scale in the core region (see Fig. 7).

5 CONCLUSIONS

The new possibilities given by the present experimental methods contribute to the knowledge in the qualitative behaviour of pipe flows of wood-fibre suspensions in at least two aspects. Firstly, unlike often phrased, for a pipe flow in mixed or turbulent flow regions (after a pump, say) the wall friction does *not* break the continuous fibre network. Instead, wall friction prevents such a network from ever forming within an annulus of some thickness or in the entire pipe. (Actual breaking of fibre network would only take place if the flow was first stopped to allow the continuous network to form, and then resumed.) Even though this difference may appear quite superficial, it can have some significance, *e.g.*, when using the measured values of disruptive shear stress of the fibre network in predicting pipe flow behaviour. It is not clear, without further investigation, that the value of disruptive shear stress measured by actually breaking an existing network by applied shear stress is the proper value to be used, *e.g.*, in predicting the transition from plug flow to mixed and turbulent flow regions in conventional pipe flows.

Secondly, the appearance of the fibre free lubrication layer in the plug flow regime is often explained by mechanical models based on shear deformation of the network induced by the wall stress, and the resulting reduction of plug diameter [16]. For a pipe flow brought about by a pump, such a model is unphysical simply because the undeformed state of the network never existed. Instead, the fibre plug formes from the fluidized state in decaying turbulence after a pump or any fluidizing device is originally of diameter slightly less than that of the pipe. The existence of lubrication layer is more likely due to inertial lift force that acts on particles moving near the wall. This phenomenon leads to a tubular pinch effect where the fibres are repelled from the wall and the fibre plug is formed in a state where the lift force is balanced by the elastic force of the network. The elastic force, in turn, is affected by the turbulent energy of fibres, partially stored as the elastic energy of the forming network.

In this experiment a forward facing step was used to induce transient flow in decaying turbulence field and the resulting approach to fully developed flow. In practical applications, turbulent flow may be generated by other devices such as pumps, mixers and valves. One can, however, expect the qualitative features of the flow remain the same irrespective of the way in which the turbulence was generated. The results presented in this paper are based on measurements with only one pipe diameter. Flows in larger pipes may involve new physical phenomena due to a large set of possible length scales, thus the results reported have to be verified with a set of different pipe diameters.

Premilinary experimental results with pipe diameters 100 mm and 200 mm are qualitatively similar to the results reported here. In addition, two new experimental methods will be available in the near future that will enable even more detailed study on the flow phenomena of wood-fibre suspensions. Both a special imaging technique and an optical coherence tomography (OCT) method will be used in studying the consistency and velocity profiles near the pipe wall. Especially, the OCT method will propably bypass the wall-proximity limitation of PUDV method, and will give us new experimental data in the submillimiter scale from the pipe wall.

REFERENCES

1. G. G. Duffy. The unique behaviour of wood pulp fibre suspensions. In 9th *International Conference on Transport and Sedimentation of Solid Particles*, September 1997.
2. P. F. W. Lee and G. D. Duffy. An analysis of the drag reducing regime of pulp suspension flow. *Tappi J.*, 59:119–122, 1976.
3. W. Brecht and H. heller. A study of pipe friction losses of paper stock suspensions. *Tappi J.*, 33(9), 1950.
4. G. D. Duffy. A review and evaluation of design methods for calculating friction loss in stock piping systems. *Tappi J.*, 59(8):124–127, 1976.
5. Møller K. and Duffy G. D. An equation for predicting transition-regime pipe friction loss. *Tappi J.*, 61:63–66, 1978.
6. TIS0410-14. Generalized method for determining the pipe friction loss of flowing pulp suspensions. Technical report, Tappi J., 1988.
7. A. Jäsberg. *Flow behaviour of fibre suspensions in straight pipes: new experimental techniques and multiphase modeling*. PhD thesis, University of Jyväskylä, Jyväskylä, Finland, 2007.
8. S. Haavisto. Private communication.
9. H. Xu and C. K. Aidun. Characteristics of fiber suspension flow in a rectangular channel. *Int. J. Multiphase Flow*, 2005.
10. F. M. White. *Fluid Mechanics*. McGraw-Hill, New York, 3rd edition, 1994.
11. G. Segré and A. Silberberg. Behaviour of macroscopic rigid spheres in poiseuille flow. part 2. experimental results and interpretation. *J. Fluid Mech.*, 14:136–157, 1962.
12. R. G. Cox and S. G. Mason. Suspended particles in fluid flow through tubes. *Ann. Rev. Fluid Mech.*, 3:291–316, 1971.
13. L. G. Leal. Particle motions in a viscous fluid. *Ann. Rev. Fluid Mech.*, 12:435–476, 1980.
14. F. Feuillebois. Some theoretical results for the motion of solid spherical particles in a viscous fluid. In G. F. Hewitt, J. M. Delhaye, and N. Zuber, editors, *Multiphase Science and Technology*, volume 4, pages 583–789. Hemisphere, 1989.

15. J. Feng, H. H. Hu, and D. D. Joseph. Direc simulation of initial value problems for the motion of solid bodies in a newtonian fluid. part 2. couette and poiseuille flows. *J. Fluid Mech.*, 277:271–301, 1994.
16. K. Møller, G. D. Duffy, and A. L. Titchener. The laminar plug flow regime of paper pulp suspenions in pipes. *Svensk Papperstidning*, (24):829–835, 1971.

NEW EXPERIMENTAL RESULTS ON THE FLOW REGIMES IN CLOSED CHANNEL FLOWS OF WOOD FIBRE SUSPENSIONS

Ari Jäsberg[1,2] and *Markku Kataja*[1]

[1]Department of Physics, P.O. Box 35 (YFL),
FI-40014 University of Jyväskylä, Finland
[2]VTT, P.O. Box 1603, FI-40101 Jyväskylä, Finland

Daniel Söderberg KTH / Innventia

I have two questions. First, if you go to your slide with the definition of turbulence intensity (section 2.1 in the paper in the proceedings, ed.). This is of course an approximation and I was wondering how you interpret it, because you are assuming parallel flow to get the velocity since the velocity profile meter does not measure direction.

Ari Jäsberg

That is true. The analysed velocity component is parallel to the axis of the pipe. We do not measure all three components. With this ultrasound measurement we get the velocity component in the direction of the ultrasound beam.

Daniel Söderberg

Yes, which means that if you had a velocity fluctuation towards the probe you would over-interpret that as a streamwise component

Discussion

Ari Jäsberg

Yes, this is not the absolute value, but a value that scales with the real value.

Daniel Söderberg

Yes, and the second question. is about the attenuation of turbulent eddies at the recirculation. It seems to be quite in accordance with what you see that the transport of turbulent kinetic energy down to viscous dissipation is hindered by having fibres and flocs. If you have the turbulent transport from large scales to small scales, and if you put in fibres and flocs, they will actually prevent the dissipation to smaller scales, which would attenuate floc motion.

Ari Jäsberg

We propose here that only the largest eddies are attenuated effectively. At fixed position inside the yield region, the size of the largest eddies is set by the distance from the pipe wall. These large eddies are attenuated effectively, but smaller ones can survive and break through the cascade towards the scale of viscous dissipation.

Daniel Söderberg

Which we really do not know?

Ari Jäsberg

Well this is a possible, a plausible reason. We have not measured the turbulence spectrum.

Daniel Söderberg

Do you think OCT would give you more data down to this small scale?

Ari Jäsberg

Well, I am not that familiar with what the time resolution is for that. I hope that it would but I am not sure.

Daniel Söderberg

Thank you.

Ilya Vadeiko FPInnovations

You showed in your study results for two different species for pine and birch, but I did not really grasp if you drew any conclusions about the effect of the species on your results.

Ari Jäsberg

We have not made any comprehensive studies on the effect of species on the flow behaviour and the physical phenomena behind it. These results were shown as an example of the capabilities of the current experimental methods in resolving the relevant physical phenomena.

Ari Kiviranta M-real (from the chair)

You showed in the beginning that there is quite a lot of potential for energy savings in pumping. Based on these results and what you have seen so far, if you could run the pumps and pipelines at their optimum point, what are the potential savings?

Ari Jäsberg

I told you about a 10–20% over-estimate in the design equations that I used in dimensioning. This over-estimate is not realized due to over-dimensioning, but the operating point migrates away from the optimum design point and the efficiency of the pumps decreases. In order to be able to give you a realistic answer, I should know the change in this efficiency – which I do not know at the moment.